Title: Adult-born hippocampal neurons undergo extended development and are morphologically distinct from neonatally-born neurons

Authors: John Darby Cole[1], Delane Espinueva[1], Désirée R. Seib, Matthew B. Cooke, Shaina P. Cahill, Timothy O'Leary, Sharon S. Kwan, Jason S. Snyder*

[1]these authors contributed equally
*corresponding author: jasonsnyder@psych.ubc.ca, 604-822-3269

Affiliation: Department of Psychology
Djavad Mowafaghian Centre for Brain Health
University of British Columbia
2211 Wesbrook Mall
Vancouver, British Columbia
Canada V6T 2B5

Running title: Protracted development of adult-born neurons

Keywords: adult neurogenesis, critical period, hippocampus, plasticity, retrovirus

Abstract: During immature stages, adult-born neurons pass through critical periods for survival and plasticity. It is generally assumed that by 2 months of age adult-born neurons are mature and equivalent to the broader neuronal population, raising questions of how they might contribute to hippocampal function in old age when neurogenesis has declined. However, few have examined older adult-born neurons, or directly compared them to neurons born in infancy. Here, we used a retrovirus to visualize functionally-relevant morphological features of 2- to 24-week-old adult-born neurons in the rat. Two-week-old neurons had a high proportion of dendritic filopodia, small presynaptic terminals and an overproduction of distal dendritic branches that were later pruned, collectively indicating immaturity. From 2-7 weeks neurons grew and attained a relatively mature phenotype. However, several features of 7-week-old neurons suggested a later wave of growth: these neurons had larger nuclei, thicker dendrites and more dendritic filopodia than all other groups. Indeed, between 7-24 weeks, adult-born neurons gained additional dendritic branches, grew a 2$^{nd}$ primary dendrite, acquired more mushroom spines and had enlarged mossy fiber presynaptic terminals. Compared to neonatally-born neurons, old adult-born neurons had greater spine density, larger presynaptic terminals, and more putative efferent filopodial contacts onto inhibitory neurons. A model of extended development predicts that adult neurogenesis contributes to the growth and plasticity of the hippocampus until the end of life, even after cell production declines. Persistent differences from neonatally-born neurons may also endow adult-born neurons with unique functions even after they have matured.

## INTRODUCTION

Morphological and physiological studies of adult-born neurons suggest that adult neurogenesis may play an important role in hippocampal function. During the first 2-8 weeks of neuronal development, adult-born neurons are less constrained by GABAergic inhibition and display greater greater afferent and efferent synaptic potentiation (Snyder et al., 2001; Schmidt-Hieber et al., 2004; Ge et al., 2007; Gu et al., 2012; Marín-Burgin et al., 2012; Chancey et al., 2013). They have greater excitability, which enables them to be recruited despite immature innervation by cortical inputs (Mongiat et al., 2009; Dieni et al., 2013). During defined windows of time they also undergo experience-dependent survival and innervation by excitatory and inhibitory neurons, and they exert greater recruitment of GABAergic interneurons (Epp et al., 2007; Anderson et al., 2010; Bergami et al., 2015; Vivar et al., 2015; Alvarez et al., 2016) . The transient nature of these unique properties has suggested that adult-born neurons have the greatest impact on circuits and behavior when they are in an immature critical period (Aimone et al., 2009; Kim et al., 2012; Snyder and Cameron, 2012).

While adult-born neurons eventually acquire features of developmentally-born neurons (Laplagne et al., 2006; Stone et al., 2011), the extent to which they are similar is unclear because few studies have examined adult-born neurons beyond the traditional critical window of ~2-8 weeks. There is evidence that even old adult-born neurons have an enhanced capacity for experience-induced morphological growth and immediate-early gene expression (Lemaire et al., 2012; Tronel et al., 2015). Additionally, studies that have characterized adult-born neurons at older ages typically have not directly compared them to neurons born in development, making it difficult to conclude whether adult-born neurons are fundamentally similar or distinct from developmentally-born granule neurons. Work that has examined neurons born at different stages of life has found differences in the rate of maturation (Overstreet-Wadiche et al., 2006; Trinchero et al., 2017), neuronal survival (Cahill et al., 2017), immediate early gene expression (Imura et al., 2018; Ohline et al., 2018), morphology and physiology (Kerloch et al., 2018; Save et al., 2018). Thus, there appears to be an ontogenetic basis for cellular heterogeneity in the dentate gyrus (DG) (Snyder, 2019).

In most mammals, neurogenesis declines approximately 90% between young and mid-adulthood and, by old age, newborn neurons are scarce (Lazic, 2012). If new neurons are particularly important during a brief window of immaturity, can neurogenesis make a significant contribution to hippocampal function later in life, when so few neurons are added? This question is important because the DG is highly-vulnerable to age-related pathology (DeKosky et al., 1996; Yassa et al., 2010) and the extent of neurogenesis in human aging is unclear (Eriksson et al., 1998; Knoth et al.,

2010; Dennis et al., 2016; Sorrells et al., 2018; Moreno-Jiménez et al., 2019). One possibility is that adult-born (or later-born) neurons may continue to mature and display developmental plasticity beyond the traditional critical period. That 4-month-old adult-born neurons display enhanced spatial learning-induced morphological plasticity (Lemaire et al., 2012) suggests that old adult-born neurons may still have "room to grow" later in life when fewer neurons are being generated. Second, protracted neurogenesis may contribute to the functional heterogeneity of the DG by producing distinct types of neurons at different stages of life (Snyder, 2019). In this way, neurons born in adulthood may mature to become distinct from neurons born in development, and may therefore offer unique functions even in old age, when neurogenesis rates have declined. To test these possibilities we used a tdTomato-expressing retrovirus to visualize the detailed morphology of various-aged DG neurons in rats. By examining dendrites, spines and presynaptic terminals, we find that adult-born neurons continue to develop, and remain morphologically-distinct from neonatally-born neurons, over an extended period of 24 weeks.

## METHODS

### Animals

Long Evans rats were bred, housed, and treated according to guidelines of the Canadian Council on Animal Care and with protocols approved by the UBC Animal Care Committee. All rats were bred and housed in the animal facility of the Department of Psychology using wild-type breeders from Charles River Canada. Rats were weaned at 21 days of age, pair housed (cages 48 x 27 x 20 cm) in same-sex colony rooms separate from breeders, and given ad libitum access to water and rat chow. Cages were kept in on a 12-hour light/dark cycle, with the light cycle starting at 9:00 am. All manipulations were conducted in the light phase.

### General experimental design

An overview of the experimental design is provided in Fig. 1. The general approach was to use a tdTomato-expressing retrovirus to birthdate cohorts of DG neurons that were either born in infancy (the day of birth; postnatal day 1) or adulthood, and enable visualization and quantification of their morphological properties. Most groups were examined when rats were 16 weeks old; retrovirus was injected at different times prior to this endpoint to examine neurons at different stages of cellular development, and to compare them to neurons born in the neonatal period. Neuronal ages were 2w (16 rats), 4w (8 rats), 7w (13 rats) and 16w (15 rats; neonatal-born), all of which were examined in 16-week-old rats. An additional cohort of adult-

born neurons was allowed to survive until 24w (7 rats), and this was the only group that was examined at a different animal age (32w).

Some animals in the 2w, 4w, 7w and 16w-neonatal groups were additionally trained for 1 day in a spatial water maze, 1 week prior to endpoint, to examine possible experience-dependent effects on structural morphology. However, since effects of water maze training were minimal, cells from control and trained rats were pooled. Morphological features of control and water maze-trained rats are provided as Extended data and do not contribute to the main conclusions of this study.

Retrovirus production

The retroviral vector used in this study was derived from a Moloney Murine Leukemia-Virus (MMLV), in which tdTomato expression is driven by a Ubiquitin (Ubi) promoter as described previously (van Praag et al., 2002). Retroviral Ubi-tdTomato (MMLV-tdTomato; kindly provided by Dr. Shaoyu Ge) and VSV-G (kindly provided by Dr. Ana Martin-Villalba) plasmids were transfected in HEK293-GP cells (kindly provided by Dr. Diane Lagace) using polyethylenimine. Retrovirus was harvested 2 and 3 days after transfection, followed by ultracentrifugation (2 h at 27,000rpm). Viral titers ranged from 0.8 to 30 x $10^4$ colony forming units/ml.

Stereotaxic retrovirus injection into the dorsal dentate gyrus

MMLV-tdTomato was injected into the DG of rats according to sterile surgical procedures approved by the UBC animal care committee. Rats were anaesthetized with isoflurane, given Ketoprofen (5mg/kg), local bupivacaine and lactated ringers (10ml/kg) every hour during the surgery. For adult surgeries, heads were levelled and fixed in a stereotaxic frame (Kopf, Tujunga, CA) and retrovirus injections were made at -4.0 mm posterior, ±3.0 mm mediolateral and -3.5 mm ventral relative to bregma. One µl of retrovirus was injected into each hemisphere, at a speed of 200 nl/min, using a 30 gauge Hamilton needle and a microsyringe pump (World Precision Instruments, Sarasota, FL). The needle remained in place for 5 min after the injection to allow the retrovirus to diffuse. For neonatal surgeries, pups were anesthetized with isoflurane, manually secured in the stereotaxic apparatus, and injected with 500 nl of retrovirus into the dorsal hippocampus (position estimated by eye, relative to lambda) over ~30 sec.

Spatial water maze training

Experimental and cage control animals from the 2w, 4w, 7w and 16w-neonatal groups were habituated to handling for 1 week prior to the start of training. Trained rats were subjected to 8 trials in a standard spatial water maze. The pool diameter was 2 m, water was 20°C and made opaque with white nontoxic tempera paint, and the

platform (10 cm in diameter) was submerged 1 cm below the surface of the water. Distal cues were located 1-3 meters away, on the room walls, providing the spatial information necessary to effectively learn to navigate the hidden platform. Acquisition performance is provided in Fig. 1-1.

Tissue processing

Animals were deeply anesthetized with isoflurane and transcardially perfused with 120 ml of 4% paraformaldehyde (PFA) in PBS (pH 7.4). Extracted brains were immersed in 4% PFA for an additional 48 hours at 4°C. Using a vibratome, brain sections were cut at 100 µm and kept in their rostro-caudal sequence to facilitate reconstruction of neurons across multiple sections. Slices were then boiled in 0.1 M citric acid for 15 minutes, and washed in PBS, and incubated in 10% PBS-TX with 3% horse serum (ThermoFisher Scientific, cat# 16050122) for 30 minutes. Sections were then incubated in rabbit anti-RFP (1:1000; Rockland cat# 600401379) with 10% PBS-TX with 3% horse serum, for 72 hours, on a shaker, at $4^0$C. Sections were then washed with PBS-TX, incubated with donkey anti-rabbit Alexa-Fluor 555 (1:250; ThermoFisher Scientific, cat# A31572) for 60 minutes at room temperature. After another PBS wash, slices were placed in DAPI diluted 1:1000 with PBS for 5 minutes. Slices were washed with PBS four more times before being mounted, serially, onto slides (Fisherbrand Superfrost Plus) and coverslipped with PVA-DABCO.

Imaging and morphological analyses

For all morphological analyses, images of tdTomato$^+$ neurons were acquired with a Leica SP8 confocal microscope. tdTomato expression was sufficiently robust in all groups to enable reliable visualization and quantification, but a higher gain was used for immature cells since intensity was weaker and their substructures tended to be thinner and smaller. Unless stated otherwise, analyses and measurements were performed on the z-stacks to accurately distinguish fine morphological details from each other and from background noise that can interfere with signals (e.g. particularly in maximum intensity projections).

For dendritic analyses, images 1024 x 1024 pixels in size and at a z-resolution of 1.25 µm were acquired with a 25x, water-immersion lens (NA 0.95) at 1x zoom. Granule cells from the suprapyramidal blade were imaged across adjacent sections to obtain the full dendritic tree. Neuronal dendrites were traced in Image J with the Simple Neurite Tracer plugin (Longair et al., 2011). The full dendritic tree (i.e. across multiple sections) was included for analyses of total dendritic length and dendritic branching order (1°, 2°, 3° etc., using the Neuroanatomy plugins for ImageJ). Sholl analyses of dendritic branching were performed on individual sections that contained ≥ 70% of the total dendritic length of a given neuron (see details in Results). Dendrite thickness was

measured from protrusion images (see below) and calculated as the average of 3 thickness measurements taken at both ends and the middle of the 30-70 μm segment. A single segment was measured from each of the inner, middle and outer molecular layers per cell.

Dendritic protrusion images were acquired with a glycerol-immersion 63x objective, at 1024 x 1024 pixels in size, 0.75 μm in z resolution, and at 5x zoom. Segments 30 μm to 70 μm in length, from cells in the suprapyramidal blade, were sampled from the inner, middle and outer molecular layers (molecular layer divided into 3 zones of equal width, approximating the terminal zones for hilar, medial entorhinal and lateral entorhinal axons, respectively). Typically, the same neurons were sampled in all 3 layers and, for total protrusion analyses, values were averaged. Protrusions, obvious elongations that extend approximately perpendicular from the dendrite, were counted with the ImageJ Cell Counter plugin. They were categorized according to morphological classes that vary with maturity (Toni et al., 2007; Berry and Nedivi, 2017): filopodia (immature, thin extensions that lack a bulbous head and are typically devoid of synapses), thin spines (putative post-synaptic spines that have a bulbous head and a thin neck), stubby spines (short and lacking a spine neck; spines with this appearance were included in protrusion density calculations but were not separately analyzed) and mushroom spine (mature, stable spines with synapses; here defined as those with a large head of ≥ 0.6 μm in diameter).

Large mossy fiber boutons (MFBs) were imaged with a glycerol-immersion 63x objective, at 1024 x 1024 pixels in size, 1 μm z resolution, and at 5x zoom. MFBs were sampled randomly within CA3a, CA3b, and CA3c and were identified by their large, irregular shape and (typically) associated filopodial extensions (Claiborne et al., 1986; Acsády et al., 1998). Cross-sectional area was measured on maximum projections of stacked images using Image J. Filopodia, protrusions from the bouton between 1 μm and 25 μm in length, were analyzed from z-stacks.

Soma and nuclear sizes were measured from the neurons that were imaged for dendritic tree analyses, from the z-plane that had the largest tdTomato$^+$ cell body and associated DAPI$^+$ nucleus, respectively (typically the middle plane of the cell).

<u>Modelling spine dynamics across the lifespan</u>

We developed a mathematical model to estimate the cumulative effects of neurogenesis throughout the lifespan, focusing on dendritic length and spine numbers as an example. Using MATLAB, we identified functions that effectively fit age-related changes in neurogenesis and the growth of dendrites and spines as adult-born neurons matured (equations and code in Fig. 7-1). Published counts of $^3$H-Thy$^+$ and BrdU$^+$ cells (Altman and Das, 1965; Schlessinger et al., 1975; Kuhn et al., 1996), that we have recently used to estimate the timecourse of neurogenesis in the rat (Snyder, 2019),

were fit with a double Gaussian function to estimate rates of neuron addition throughout life. We did not correct for inflated counts due to redivision of labelled precursor cells since: 1) embryonic and perinatal datasets were limited to heavily-labelled granule neurons, thereby largely excluding cells that would be labelled due to redivision (Schlessinger et al., 1975)), 2) inflation due to redivision in adulthood will be approximately offset by death of immature neurons (redivision causes ~2x increase in labelled cells (Cameron et al., 1993), death removes ~1/2 of cells (Snyder et al., 2009)). The total (unilateral) granule cell population was fixed at 1.2 million cells (West et al., 1991), and 1 existing neuron (born before P56) was removed for each adult-born neuron that was added (Dayer et al., 2003; Cahill et al., 2017). For adult-born neurons, age-related increases in dendritic length and mushroom spines were fit with power functions and thin+mushroom spines were fit with a sigmoidal function. We then integrated dendrite and spine growth functions for all neurons born between P56 and P730 to predict morphological consequences of neurogenesis in adulthood. Dendrite lengths and spine densities for neurons born prior to adulthood were fixed at levels observed in P1-born neurons.

Statistical Analyses

Neuronal morphology varied substantially, even within the same animal. To retain these details, and compare subpopulations of neurons of the same age, we performed most analyses at the level of the structure of interest (i.e. cell, bouton), except where indicated otherwise. Morphological differences between different-aged neurons were typically assessed by ANOVA with Holm-Sidak post-hoc comparisons. Samples that were not normally distributed were log transformed prior to statistical analyses and, if distributions remained non-normal, the untransformed data were analyzed by a non-parametric Kruskal-Wallis test with post-hoc comparisons by Dunn's test. All graphs show non-transformed data. In all cases, significance was set at $\alpha = 0.05$.

## RESULTS

Dendrites

Consistent with previous reports, the dendritic tree of adult-born neurons matured over several weeks (Fig. 2). Two and 4-week-old neurons had noticeably thinner and more irregular-shaped dendrites that often did not extend to the hippocampal fissure. By 7 weeks, dendrites were thicker, longer and, at even older ages, tips of dendrites often curved sideways upon approaching the hippocampal fissure (Fig. 2-1). While less common than in younger cells, early-terminating dendrites (Fig. 2a) and thin, spine-poor dendritic segments (Fig. 4a) were also observed on 7-

and 24-week-old neurons, suggesting the presence of immature processes and continued growth.

To determine the timeframe of growth of adult-born neuron dendrites, dendritic lengths were measured in their entirety, across sections. Water maze training did not alter dendritic length (Fig. 2-2) and so cells of the same age were pooled. The total number of cells examined were: 2w: 76 cells (16 rats), 4w: 49 cells (8 rats), 7w: 65 cells (13 rats), 24w: 37 cells (7 rats), 16w-neonatal: 74 cells (15 rats). Among adult-born cells, dendritic length increased from 1954 μm at 2 weeks to 3105 μm at 24 weeks (Fig. 2b). There was greater net dendritic growth at younger cell ages; from 2-4 weeks there was a net increase of 392 μm (28 μm/day) whereas over the much longer interval of 4-24 weeks there was only an additional 759 μm of growth (4 μm/day). Neonatally-born neurons had an average total dendritic length of 3565 μm; this was greater than all adult-born neuron groups, though populations overlapped. To obtain a complementary measure of dendritic growth, we measured the width of dendrites in the inner, middle and outer molecular layers (Fig. 2c). Dendrite thickness doubled between 2-7 weeks (0.5 to 1.0 μm) and then decreased slightly by 24w, which was thinner than 16w-neonatal neurons. Consistent with theoretical predictions that dendrites taper to optimize current transfer (Bird and Cuntz, 2016), dendritic thickness decreased from the inner to middle to outer molecular layers, and this did not vary across cell age.

Dendritic branching patterns change as adult-born neurons develop (Kerloch et al., 2018) and their precise morphology likely determines the strength and integration of synaptic inputs from different pathways (Spruston, 2008). We therefore conducted a Sholl analysis and quantified the number of dendritic intersections at concentric 10 μm intervals from the cell body through the molecular layer. Our initial analysis included all cells that had at least 40% of the dendritic tree length in the analyzed section, and suggested that older-adult-born neurons had more intersections at distal dendritic regions. However, these results were biased by the larger number of cut dendrites in the 16w-neonatal group relative to the adult-born neuron groups. We therefore excluded cells where < 70% of the total dendritic length was present in the analyzed section, and found 10-30 neurons per group that fit this criterion. Younger cells still tended to have more complete neurons but group differences were not statistically significant (% of neuron present in analyzed section: $F_{4,88}$=2.6, P=0.04; post-hoc comparisons all P>0.05; number of cut dendrites: $F_{4,88}$=3.1, P=0.02; post-hoc comparisons all P>0.05). The Sholl analysis revealed that the number of dendritic branch intersections increased at progressively greater distances from the cell soma (Fig. 2d). Neonatal-born neurons had more intersections than adult-born groups at proximal dendritic regions, reflecting their positioning in the superficial granule cell layer, closer to the inner molecular layer. Immature, 2w cells had fewer dendritic

intersections in proximal and distal regions, but were not different from the other groups in the intermediate dendritic tree. Proximal and distal dendritic intersections continued to increase from 4-7 weeks of cell age, at which point adult-born neurons were comparable to neonatally-born neurons, aside from having fewer intersections at the proximal dendritic tree.

To obtain a complementary measure of dendritic structure that is independent of the absolute length and positioning of the cell body and branches, and is not influenced by tissue sectioning, we quantified the total number of dendritic branches across the full dendritic tree (Fig. 2e). Consistent with recent in vivo and in vitro results (Gonçalves et al., 2016; Beining et al., 2017; Jungenitz et al., 2018), we observed significantly greater numbers of dendritic branches in immature cells. 2w cells had the most dendritic branches; there was significant pruning of branches from 2-4w, which persisted to 7w. However, the total number of dendritic branches then increased between 7w and 24w, indicating a later wave of dendritic growth in adult-born neurons.

To identify where dendritic branching differed, we quantified branching according to order, where primary branches are those that emanate directly from the cell body, and the order increases by 1 with each branch point (Fig. 2f). Dendrites typically bifurcated at branch points but trifurcation was also observed in all groups except the 24w group. Overall, 13% of cells trifurcated (2w: 16/77 cells; 4w: 6/49 cells; 7w: 7/64 cells, 24w: 0/37 cells; 16w-neonatal cells: 14/73 cells; examples in Video 2-1). Consistent with the Sholl data, the number of lower-order (1°-3°) branches increased as adult-born cells aged and, by 24w, was comparable to neonatally-born cells. Adult-born neurons are commonly recognized to have a single primary dendrite, which we observed in 2-7w cells. However, by 24w adult-born cells had, on average, 2 primary dendrites. Quaternary branches were the most common, and did not differ across groups. Whereas the number of lower order dendrites correlated with cell age, the number of higher order dendrites tended to show the opposite pattern. 2w cells had significantly more high-order branches (5°, 6°) compared to all other groups. Neonatal-born neurons had the fewest higher order branches, though this was only significant for 5° branches.

Finally, we calculated the branching index of cells, a measure that normalizes dendritic branching to the number of primary dendrites (branch tips / # primary dendrites; Fig. 2g). The branching index was greater in 2w cells than all other groups. In older cells, the distribution of branching indices tended to be bimodal; cells with a single primary dendrite had a branching index that was ~twice that of cells with ≥ 2 primary dendrites. When we excluded cells that had more than one primary dendrite, 2w cells still had a greater branching index than older-aged cells, indicating that their

greater branching index is due to more extensive distal branching and not simply because they tend to only have 1 primary dendrite.

Our branch order analyses raise the question of how adult-born neurons gain additional primary dendrites. A second primary dendrite could be generated de novo from the cell body or it could arise by branching off of the existing dendritic tree. It seemed unlikely that additional primary dendrites arise via sprouting because, out of 294 cells examined, only 4 cells possessed an unbranched primary dendrite and only 1 of these cells was adult-born (24w). We therefore hypothesized that new primary dendrites may emerge from the existing dendritic tree, via an "unzipping" of the primary dendrite until the first branch point meets the soma. Indeed, amongst cells with a single primary dendrite, we found a significant shortening between 2 and 4 weeks (Fig. 3a). There were no further changes, possibly because the cells with the shortest primary dendrites become excluded from the analysis as they mature and gain a second primary dendrite.

From 2-24 weeks there was a gradual transition from cells having only a single primary dendrite to having 2 or more primary dendrites (Fig. 3b). Since the biggest transition occurred between 7-24 weeks, we focussed on 7 weeks for further analyses. We reasoned that, if primary dendrites "unzip", there should be similar patterns of branching in cells with 1 vs 2 primary dendrites. Indeed, when we excluded the primary dendrite from cells with only 1 primary dendrite (1P), the branch order pattern became identical to cells that had 2 primary dendrites (2P; Fig. 3c). We then examined the branch index and total length of 1°-branch-trees (i.e. trees associated with a primary dendrite; 1P cell will have one, and 2P cell will have two, 1°-branch-trees). For both measures, 1°-branch-trees of 1P cells were double that of 2P cells, consistent with a model where unzipping a longer, more complex 1°-branch-tree results in 2 simpler 1°-branch-trees (Fig. 3d). However, 1°-branch-trees had a much greater range and were more variable in 2P cells, suggesting possible within-cell variation in 1°-branch-tree complexity (branch index coefficients of variation (CV): 2P cells: 45%, 1P cells: 14%; length CVs: 2P cells: 34%, 1P cells: 18%). If 2P cells have one 1°-branch-tree that is less developed than the other this could either be due to immaturity (supporting a sprouting model) or it could be an innate property that existed prior to unzipping. If innate, then differences in dendritic complexity should be apparent in the 2°-branch-trees of 1P cells that have not (yet) unzipped. To test this, we compared the branching order, branch index and total length of 1°-branch-trees (2P cells) and 2°-branch-trees (1P cells; Fig, 3e-i). For all measures, there was within-cell variation where a "high" branch-tree had significantly greater complexity and length compared to a "low" branch-tree. This pattern was observed in both 1P cells and 2P cells, supporting a model where inherent differences in dendritic sub-trees exist before a primary dendrite unzips to form 2 primary dendrites in an adult-born neuron (Fig. 3j). Further, the

average and minimum total lengths of "low" 1°-branch-trees on 2P cells were 1012 μm and 499 μm, respectively. To sprout trees of these lengths from 4-7w, dendrites would have to grow at rates of 48 and 15 μm/day, respectively, which is unlikely given that the average rate of dendritic growth for the *entire* dendritic tree over this interval was only 15 μm/day.

Spines

To assess putative postsynaptic targets of cortical and subcortical axons, protrusion densities on DG neurons were quantified throughout the molecular layer (Fig. 4). Water maze training had minimal impact on protrusion densities and so data from cells of the same age were pooled (Fig. 4-2). There were few protrusions on 2w cells (0.2/μm) but a dramatic 500% increase between 2-4w and a further 80% increase from 4-7w. Total protrusion densities did not increase further between 7w and 24w, but plateaued at levels that were ~60% greater than neonatally-born neurons (Fig. 4b). Distinct inputs are segregated along granule neuron dendritic trees, where the lateral entorhinal cortex targets the outer molecular layer, the medial entorhinal cortex targets the middle molecular later, and subcortical and commissural fibers target the inner molecular layer (Leranth and Hajszan, 2007; Witter, 2007). We therefore examined whether the maturational profile of postsynaptic sites differs along these functionally-relevant anatomical subregions and found fewer protrusions in the inner molecular layer at 4 and 7 weeks of age (Fig. 4c). This regional difference was absent by 24 weeks of age and not present in neonatally-born neurons, suggesting delayed maturation of commissural and/or subcortical inputs onto adult-born neurons. Consistent with these data, protrusion density was generally not different across dendritic branch orders, except for 2w and 4w cells, which had lower densities on primary and secondary branches compared to their higher order branches (Fig. 4d).

Spines can be categorized into functionally-relevant subclasses based on morphology, where thin filopodial protrusions tend to be transient, plastic potential synaptic partners and large mushroom spines are structurally stable, synaptically stronger, and believed to be sites of long-term information storage (Holtmaat and Svoboda, 2009; Berry and Nedivi, 2017). Consistent with a developmental role, filopodia density peaked at 7 weeks (Fig. 4e). The density of thin spines followed the same pattern as the protrusion densities, and accounted for most of the protrusions (Fig. 4f). We additionally quantified large mushroom spines in different-aged DG neurons (Fig. 4g). Whereas mushroom spines were virtually absent from young 2-week-old cells, they steadily increased with age. At 24 weeks, densities of mushroom spines were greater than all other groups and they were nearly twice as common as in neonatally-born neurons. The regional distribution of mushroom spines resembled the overall spine density pattern, where fewer mushroom spines were found in the inner

molecular layer on 4- and 7-week-old neurons (Fig. 4h). Here, however, there were also fewer mushroom spines observed on neonatally-born neurons in the inner molecular layer. While water maze training generally did not impact neuronal morphology, in the inner molecular layer, training increased spine density and it increased mushroom spine density specifically in 7w cells, suggesting accelerated development (Fig. 4-2). Examining the changes in proportion of spine type revealed a clear maturational profile, where filopodia made up the largest proportion of protrusions at 2 weeks and declined with age; mushroom spines followed the opposite pattern (Fig. 4i).

Presynaptic terminals

Dentate granule neuron MFBs are large excitatory presynaptic structures, composed of multiple active zones that target CA3 pyramidal neurons and mossy cells (Chicurel and Harris, 1992; Rollenhagen et al., 2007). Associated with each MFB are smaller filopodial extensions that form synapses with inhibitory neurons (Acsády et al., 1998). To gain insights into the role that cell age may play in efferent connectivity, we first quantified the maximal 2D area of MFBs as an anatomical proxy for synaptic strength. Water maze training did not alter MFB size and so data for boutons of the same age were pooled (Fig. 5-1). Among adult-born neurons, MFBs doubled in size between 2-7w, with most growth occurring between 4-7w. However, they grew an additional 20% between 7w and 24w. At 24w, adult-born MFBs were 34% larger than 16w-neonatal-born neurons (Fig. 5b). Across all cell populations, MFBs were smaller in CA3c than in CA3a/b (Fig. 5-2a).

We next examined the filopodial processes that protrude off of MFBs and contact GABAergic interneurons. There was an age-related increase in filopodia/MFB from 1.4 filopodia/MFB at 2 weeks to 4-5 filopodia/MFB at 7/24 weeks, which was significantly greater than that of neonatally-born cells (3.4; Fig. 5c). There were also fewer filopodia/MFB in CA3a, an effect that was driven by 4w and 7w cells (Fig. 5-2b). While young 2-week-old cells had few filopodia/MFB, their filopodia were significantly longer than those of older adult-born and neonatally-born neurons (Fig. 5d). Filopodial length declined from a mean of 7 μm at 2 weeks to ~5μm at 7 weeks of age, which was not different from 24-week-old adult-born neurons. Filopodia length of neonatally-born neurons was shorter than all adult-born populations. Filopodia were longer in CA3c than in CA3a, an effect that was not specific to any subpopulation of cells (Fig. 5-2c).

In addition to age-related changes in MFB size, there were also differences in the positioning of MFBs relative to the axon (Fig. 5e). Young adult-born cells, 2-4 weeks old, tended to have *en passant* MFBs that were located directly on the axon. In contrast, 30-40% of MFBs on older adult-born cells and neonatally-born cells were connected to the axon by a branch. Branch lengths were not different between groups, and averaged 8 μm across all cells examined. 75% of branches were less than 10 μm in

length; the longest branch was 52 μm. No obvious differences were observed in branching across CA3 subregions, but our regional sample sizes were too low to conduct a proper comparison. Water maze training did not alter the number or length of MFB filopodia (Figs. 5-3, 5-4).

Soma and nuclear size

Our analyses indicate an extended developmental trajectory for adult-born neurons, where several morphological features ultimately surpass developmentally-born neurons in size. We therefore tested the generality of our findings by measuring the size of the cell soma and nucleus, both of which vary as adult-born neurons mature (Kirn et al., 1991; van Praag et al., 2002; Amrein and Slomianka, 2010; Radic et al., 2015; Moreno-Jiménez et al., 2019); Fig. 6). Consistent with early growth, the cell soma increased in size from 2-7 weeks and was stable thereafter and similar to neonatal-born neurons. In contrast, the nuclear size was generally smaller in adult-born cells than neonatal-born cells, except at 7 weeks when adult-born cells had larger nuclei that matched 16w-neonatal cells in size.

Modelling the cumulative effects of neuron addition and extended maturation

Given the dramatic decline in neurogenesis with age, it has remained unclear whether new neurons contribute to the function of the aging brain. Our results indicate that, in addition to the cumulative effects of low rates of neurogenesis, extended growth may contribute to the plasticity of the aging brain. To test this we created a model that integrated rates of cell addition, rates of dendritic growth and rates of spine growth (see methods and Fig. 7-1). Consistent with previous estimates based on different datasets (Snyder and Cameron, 2012), and evidence from Glast CreERT2 mice (DeCarolis et al., 2013), our model predicts that ~50% of total DG neurons are added in adulthood (Fig. 7a). This translates to ~2 km of dendrite and nearly 4 billion spines (Fig. 7b). While neurogenesis in our model ended by 1.5 years, adult-born neurons continued to add to the total dendrite length and total number of spines in the DG; this was particularly salient for mushroom spines (Fig. 7b-d). Between 1-2 years we estimate that adult neurogenesis adds only 2.5% of total cells, consistent with previous quantitative estimates of neurogenesis rates later in life (Lazic, 2012), but during this time it contributes 7% of total dendritic length, 10% of total spines and 24% of mature mushroom spines in the DG (summary statistics in Table 7-1).

## DISCUSSION

Here we report that functionally-relevant morphological features of adult-born neurons develop over a surprisingly long timeframe. At 2 weeks, adult-born neurons

were underdeveloped in all respects: dendrites were thin and had a small number of protrusions, of which a relatively large proportion were filopodia. Presynaptic mossy fiber terminals were small and had few filopodial extensions. The dendritic tree, while smaller in size, had a more extensive branching pattern than older adult- and neonatal-born cells, reflecting the transient overproduction of dendritic branches. Between 2-4 weeks, all morphological features underwent growth but the greatest changes were in dendritic protrusions/spines (over 4x increase) and the number of MFB filopodia (1.5x increase). Several morphological features displayed transient peaks at 7 weeks, suggesting a distinct wave of development at this age: dendrites were thickest, nuclei were largest, and dendritic filopodia were present in greatest numbers. Between 4-7 weeks neurons displayed the greatest increase in bouton size, relative to other stages. Also, spine density and the number of bouton filopodia increased beyond the levels observed in neonatal-born neurons. By 24 weeks, adult-born neuron growth had stabilized to some extent, but there were notable changes relative to 7 weeks: neurons gained an additional primary dendrite, more total dendritic branches and greater total dendritic length. The distribution of spine types assumed a more mature phenotype (fewer filopodia, more mushroom spines) and the size of mossy fiber boutons increased a further 20%. Ultimately, compared to neonatal-born neurons, 24-week-old adult-born neurons had more dendritic protrusions (by 63%), more mushroom spines (92%), larger presynaptic terminals (34%) and more bouton-associated filopodia (33%). These differences cannot be explained by differences in cell age, where adult-born neurons had more time to mature, since adult-born cells already had greater spine densities, larger MFBs, and more MFB filopodia at 7w. Also, since neonatally-born cells mature faster than adult-born neurons (Overstreet-Wadiche et al., 2006; Zhao et al., 2006), and are needed to support behavior within weeks of their birth, it is likely that they reach a fully mature state much earlier. Indeed, developmentally-born granule neurons do not acquire any additional primary dendrites between 7-180 days and do not undergo additional dendritic growth between ~5-6 weeks to 26 weeks of age. While physiological experiments are needed to determine functional significance, our results indicate that adult-born neurons are plastic well beyond the traditional critical window and may make unique contributions to hippocampal functioning for the lifespan of the cell.

<u>Minor effect of water maze training on neuronal morphology</u>

Spatial water maze over multiple days induces morphological and electrophysiological plasticity in adult-born neurons (Ambrogini et al., 2010; Tronel et al., 2010; Lemaire et al., 2012). Since the hippocampus is essential for remembering brief experiences (Feldman et al., 2010) and adult-born DG neurons show rapid changes in spine morphology following electrical stimulation (Ohkawa et al., 2012;

Jungenitz et al., 2018), we investigated whether a single session of water maze training would be sufficient to promote morphological plasticity in DG neurons. However, effects were small and limited to inner molecular layer spines. The most robust effect was the increase in mushroom spine density at 7w, suggesting that learning accelerates the development of mature synapses in this subregion. Thus, while a short bout of experimenter handling+spatial learning may induce a small amount of structural plasticity in the DG, more extensive training appears necessary to reveal differences between neurons of different age and born at different stages of the lifespan.

Extended growth of adult-born neuron dendrites

Consistent with previous reports we observed dramatic dendritic growth in young adult-born neurons (here, 2-4 weeks old). At 2 weeks, adult-born neurons had the greatest number of branches due to the transient overproduction of distal, high-order branches that has been previously described in vivo (Gonçalves et al., 2016) and in vitro (Beining et al., 2017). While branches were pruned between 2-4 weeks and stable in number between 4-7 weeks, dendrites continued to elongate during this interval. After 7 weeks, the total number of branches and their length increased at a more modest but significant rate, in contrast to the static dendritic morphology of neurons born in early development (Kerloch et al., 2018). Why has the continued growth of adult-born neuronal dendrites not been reported previously? This is likely to be partly due to the use of markers or reporters that are only expressed during immaturity, or analyses of genetically-labelled neurons at only young cell ages (Shapiro et al., 2007; Wang et al., 2008; Leslie et al., 2011; Piatti et al., 2011; Dieni et al., 2013). While some studies have examined dendrites at later ages, analyses did not extend beyond ~8-11 weeks (Sun et al., 2013; Gonçalves et al., 2016; Beining et al., 2017; Trinchero et al., 2017). Cut dendrites may have obscured growth in some cases. Also, our extended interval of 17 weeks likely facilitated detection of cumulative growth that was not detectable over shorter intervals of days and weeks in previous studies. It remains an open question whether adult-born neurons continue to grow beyond 24 weeks.

Whereas the dendritic length data suggests a long-term plasticity function for adult-born neurons, the branching pattern matures to become broadly similar to neonatally-born neurons. Typically, adult-born neurons are considered to have only a single primary dendrite but, by examining the pattern of low order branching at early and late ages, our data suggests an "unzipping" model where the first branch point of the primary dendrite moves closer to the soma with age (or the soma moves towards the first dendritic branch). Subtrees with variable length and branching complexity also suggest the presence of different computational compartments within the granule cell dendritic tree (Losonczy et al., 2008). While 24w adult-born neurons and 16w neonatal

neurons averaged 2 primary dendrites, there was substantial variation with older adult and neonatal neurons often having 1, 2 or 3 primary dendrites. At least some mature neurons, born neonatally or in adulthood, therefore have morphological features of highly-active granule neurons (few primary dendrites and extensive higher-order branching (Diamantaki et al., 2016)).

Prolonged maturation and high density of dendritic spines

The gradual loss of immature filopodia and acquisition of mature mushroom spines is consistent with previous evidence that spine morphology changes with adult-born cell age (Toni et al., 2007). While the inner molecular layer is the site of the first synapses onto adult-born neurons (Chancey et al., 2014), our data suggests that synaptic maturation in this region is subsequently delayed until after 7 weeks but can be accelerated by a single day of water maze training (note another report that spine density is lower in the inner molecular layer regardless of cell age (Jungenitz et al., 2018)). While most studies have only analyzed spines on immature neurons, or neurons of a single age, there are several reports that spine density increases beyond 1 month of age in rodents (van Praag et al., 2002; Zhao et al., 2006; Jessberger et al., 2007; Toni et al., 2007; Jungenitz et al., 2018; Bolós et al., 2019). Furthermore, spatial water maze training can promote spine growth in 4-month-old neurons (Lemaire et al., 2012), and enriched environment from 2-6 weeks promotes spine growth and connectivity that persists at 13 weeks of cell age (Bergami et al., 2015). Thus, adult-born neurons exhibit forms of maturation-related structural plasticity that extend well beyond the timeframe when they have greater excitability and long-term potentiation. Since most adult-born neuron spines contain synapses (Toni et al., 2007), it will be important for future studies to investigate how these structural differences translate into physiological recruitment by afferent pathways.

Golgi studies of mice, primates and humans have identified a subpopulation of DG granule neurons that display ~2x the normal density of dendritic spines (Williams and Matthysse, 1983; Seress and Frotscher, 1990; Seress, 1992). Here we describe a similar phenomenon in rats and suggest that these spine-rich neurons are those generated in adulthood. The relatively high spine density of adult-born neurons has likely gone unnoticed because few studies have examined adult-born neurons at old ages, and even fewer have directly compared them to developmentally-born neurons. One study conducted a detailed examination of the maturational timecourse of stimulation-induced spine plasticity in retrovirally-labelled adult-born neurons vs AAV-labelled DG neurons (Jungenitz et al., 2018). Interestingly, the older adult-born neurons tended to have more spines than the AAV-labelled neurons, consistent with our data. However, since AAV labels DG neurons indiscriminately, the lower spine density of developmentally-born neurons could have been obscured AAV-labelled

adult-born neurons. To our knowledge, the only other study that used retrovirus to compare spine densities of developmentally- and adult-born neurons is Toni et al. (2007). While they also reported an extended period of spine formation and maturation, spines densities on old adult-born neurons (180 days) and developmentally-born (P4) neurons were similar. The reason for this discrepancy is unclear but, in addition to species and sex differences between studies, it is possible that by labelling neurons born on P1 in rats we targeted a different subpopulation of developmentally-born DG neurons than Toni et al., who labelled neurons born on P4 in mice. While this difference in timing may appear small, there are significant morphological and functional differences between DG neurons born only days apart in early development (Kerloch et al., 2018; Save et al., 2018), which may be amplified by the earlier development of the mouse DG compared to the rat (Angevine, 1965; Schlessinger et al., 1975).

Protracted growth of large mossy fiber boutons on adult-born neurons

Mossy fiber boutons are large multisynapse complexes that contact the proximal dendrites of CA3 pyramidal neurons (Amaral and Dent, 1981; Chicurel and Harris, 1992; Rollenhagen et al., 2007) and are believed to play a dominant role in recruiting ensembles of CA3 pyramidal neurons during memory formation (Rolls, 2010). Indeed, a single mossy fiber input can induce firing of postsynaptic pyramidal neurons (Henze et al., 2002; Vyleta et al., 2016). Detailed morphological investigations have found that MFB size is highly variable but increases with animal age (Amaral and Dent, 1981; Rollenhagen et al., 2007), and retroviral studies have found that MFB size, the number of active zones and the number of synaptic vesicles increases as adult-born cells mature over 2-10 weeks of age (Faulkner et al., 2008; Toni et al., 2008; Restivo et al., 2015; Bolós et al., 2019). Since larger MFBs have more active zones and elicit larger EPSPs (Galimberti et al., 2006; 2010), adult neurogenesis likely contributes to the heterogeneity of synaptic strength at the DG-CA3 synapse. Furthermore, given that extended MFB maturation ultimately results in terminals that are larger, adult-born synapses may grow to become stronger than those of developmentally-born neurons.

Generally, MFBs were smallest in CA3c, suggesting that these pyramidal neurons, which lack recurrent collaterals and tend to perform pattern separation rather than completion (Lee et al., 2015), may receive slightly weaker inputs from the DG. Other reports have identified heterogeneous experience and age-related plasticity of MFBs, where a small fraction of "core" MFBs within an individual axon undergo selective growth and branching of satellite MFBs (Galimberti et al., 2006; 2010). We did not keep track of parent axon identity, precluding a similar analysis. However, the size of 24-week-old MFBs was not normally distributed and a subset of MFBs (~50% of the population) was noticeably larger than the majority of MFBs on neonatal-born neurons.

Given that adult-born neurons initially share CA3 spines with existing neurons before developing fully independent synapses (Toni et al., 2008), their continued growth is consistent with the possibility that adult-born neurons (out)compete with developmentally-born neurons for CA3 connectivity, which may facilitate the turnover of memory (Akers et al., 2014).

We observed a significant proportion of MFBs that were not directly attached to the main axon but instead were attached to a small branch. The proportion of branched boutons increased with cell age, perhaps explaining why they have not been extensively described in previous reports that commonly focus on younger animals. Similar "terminal boutons" in the neocortex are more morphologically plastic than *en passant* boutons that are directly embedded in the axon (De Paola et al., 2006), suggesting that branched boutons may play a unique role in hippocampal function. Branching is likely to influence signal propagation and coding properties of axons (Ofer et al., 2017). Given that voltage-gated channels are differentially distributed across axonal compartments, branches could also offer an anatomical substrate for modulating the active properties of mossy fibers (Engel and Jonas, 2005; Kole et al., 2008; Rowan et al., 2016).

Thin filopodial protrusions extend off of MFBs to excite inhibitory interneurons and display distinct forms of transmission and plasticity compared to pyramidal neuron synapses (McBain, 2008). Granule neurons form more connections with efferent inhibitory neurons than pyramidal neurons (Acsády et al., 1998) and adult-born neurons play an important role in recruiting inhibitory networks (Drew et al., 2015; Restivo et al., 2015). Consistent with these data, we found that the number of filopodia per MFB plateaued at 7 weeks and remained greater than developmentally-born neurons at 24 weeks. Thus, adult-born neurons may play a long-term role in shaping inhibition in CA3, which could promote memory precision (Ruediger et al., 2011; Guo et al., 2018) by reducing overlap between neuronal ensembles (Niibori et al., 2012).

<u>Functional significance of extended development</u>

Critical periods endow adult-born neurons with a unique capacity for experience-dependent plasticity during their immature stages. However, the focus on immature neurons has come at the expense of understanding the capacity of older neurons to undergo plasticity, and led to the assumption that adult-born neurons lose their functional relevance with age (Snyder, 2019). By integrating the extended growth of adult-born neurons into a model of neuronal accumulation, we present evidence that neurogenesis makes a dramatic contribution to the overall structural plasticity of the dentate gyrus. Our model predicts the addition of 600 million spines (10% of the total) between 1-2 years, and 150 million spines (2.5% of the total) between 1.5-2 years, which is after cell proliferation has ended. Since human granule neuron dendrites

grow throughout middle to old age (Flood et al., 1985; Coleman and Flood, 1987), and neonatally-born neuron dendrites in mice do not grow over similar intervals (Kerloch et al., 2018), this suggests that adult-born neurons may offer a unique reserve of plasticity in aging, when the medial-temporal lobe becomes vulnerable to pathology (Leal and Yassa, 2015).

Plasticity aside, our data raise the possibility that adult-born neurons are functionally distinct from neurons born at other stages of life, even after they have "matured". The significantly greater spine density suggests that adult-born neurons may be inherently more likely to associate, and be recruited by, cortical inputs. The presence of larger boutons suggests that adult-born neurons may be more capable of depolarizing postsynaptic pyramidal neurons, and the presence of more filopodia suggests they may be more effective at refining CA3 representations through feedforward inhibition. Persistent differences in immediate-early gene expression are consistent with the possibility that adult-born neurons are functionally distinct from neurons born earlier in life (Tronel et al., 2015; Todorova et al., 2017; Imura et al., 2018; Ohline et al., 2018). Given cellular heterogeneity in vulnerability to disease, protracted neurogenesis may also result in subpopulations of cells that are differentially susceptible to pathology (Snyder, 2019).

## ACKNOWLEDGEMENTS

This work was supported by the Natural Sciences and Engineering Research Council of Canada, the Canadian Institutes of Health Research and the Michael Smith Foundation for Health Research.

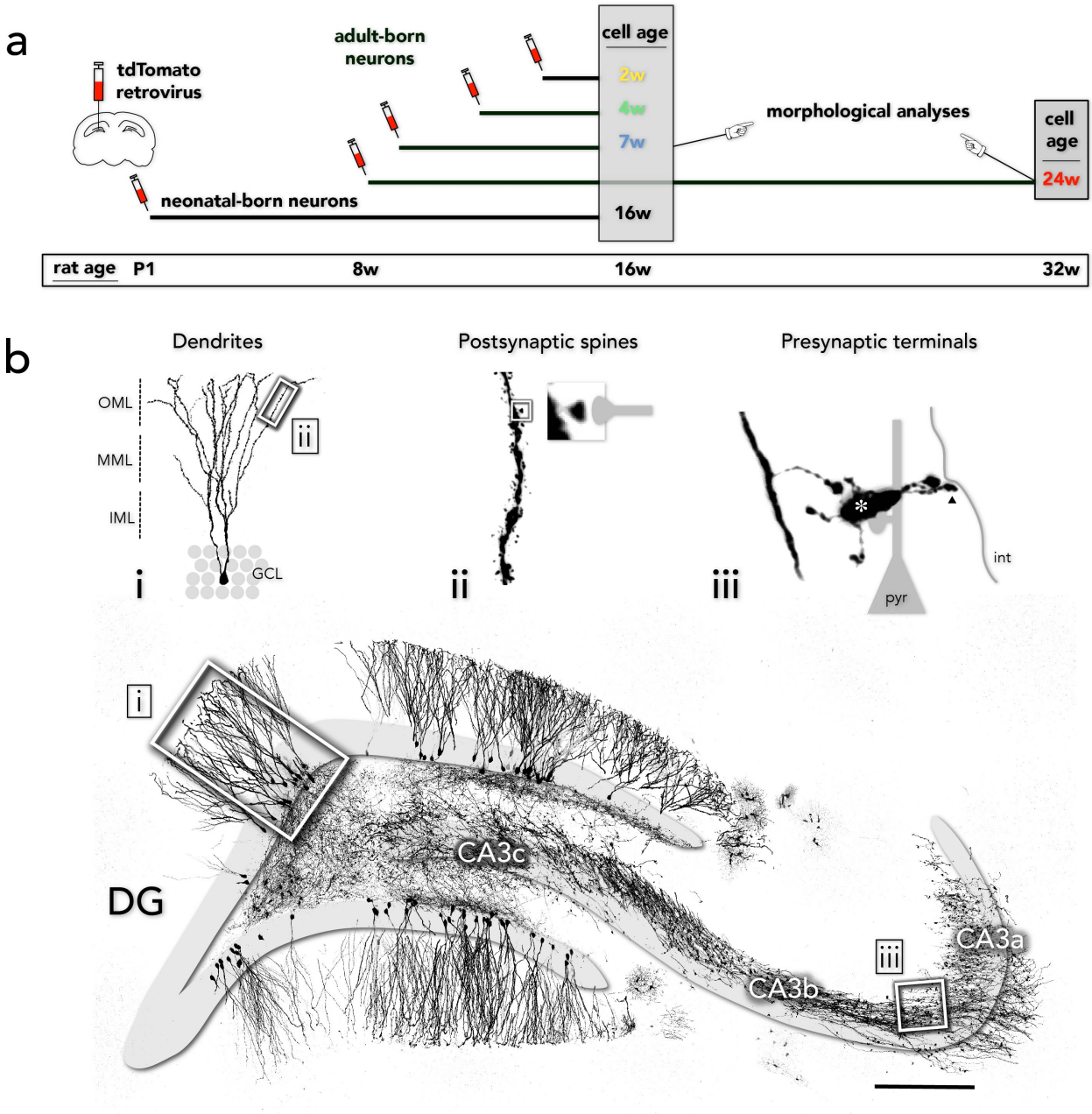


Figure 1: Experimental design. a) Timeline: tdTomato-expressing retrovirus was injected into the DG of rats to birthdate granule neurons and visualize their morphological features. All groups were examined when rats were 16 weeks of age, except one cohort of adult-born cells that were allowed to mature for 24 weeks (rat age 32 weeks). b) The large low magnification confocal image shows retrovirally-labelled, 24-week-old neurons in the dorsal hippocampus; granule and CA3 pyramidal cell layers were traced from DAPI$^{+}$ principal cell nuclei. Insets highlight the morphological features of DG neurons that were investigated: i) dendritic trees; ii) spines; iii) presynaptic mossy fiber boutons (*), which target CA3 pyramidal neurons (pyr), and filopodial terminals (arrowhead), which target inhibitory interneurons (int). OML, outer molecular layer; MML, middle molecular layer; IML, inner molecular layer; GCL, granule cell layer. Scale bar, 500 μm.

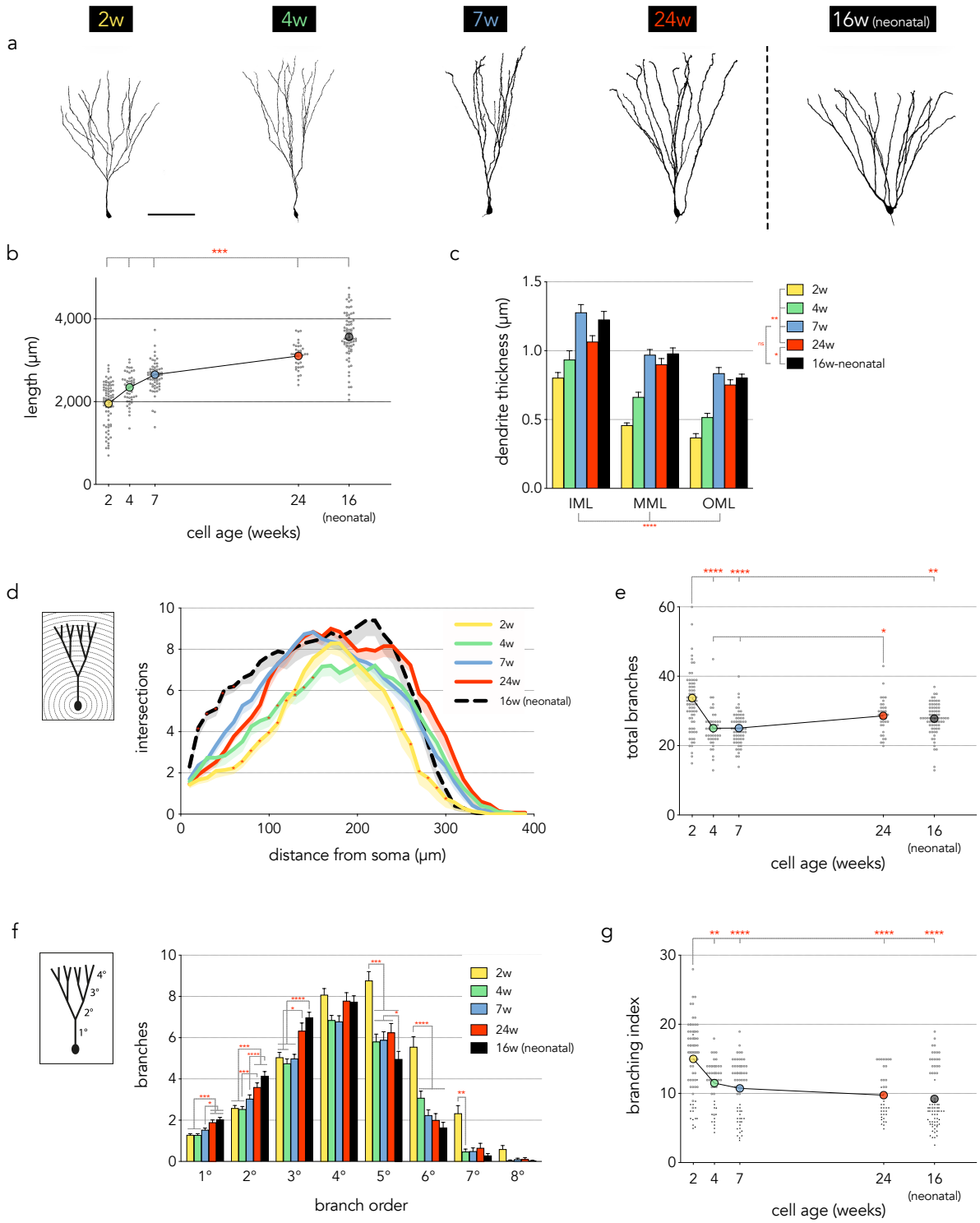


Figure 2: Dendritic structure of neonatally-born neurons and developing adult-born neurons. a) Representative confocal images of fully reconstructed dendritic trees; additional examples in Fig. 1-2. Scale bar, 100 µm. Examples of trifurcating dendrites in Video 2-1. b) The total dendritic length of adult-born neurons increased from 2 to 24 weeks and remained less than neonatally-born neurons ($F_{4,296}$=120, P<0.0001; ***P<0.001 for all group comparisons). Colored symbols indicate group means, small circles indicate dendritic lengths of individual neurons. c) Dendrites became thicker with increasing adult-born

neuron age, with the exception that 7w cells had thicker dendrites than 24w cells. Neonatally-born cells had thicker dendrites than 24w adult-born neurons. Dendrite thickness varied such that OML < MML < IML (repeated measures, mixed effects model; effect of cell age $F_{4,260}$=52, P<0.0001; effect of molecular layer region, $F_{1.7, 402}$=142, P<0.0001; cell x layer interaction, $F_{8,477}$=0.9, P=0.5). d) Sholl analyses revealed distinct patterns of dendritic complexity across cell ages (effect of cell age $F_{4,88}$=16, P<0.0001; cell age x dendritic subregion interaction $F_{120,2640}$=2.6, P<0.0001; 10-300 μm analyzed since cells did not reliably extend beyond 300 μm in all groups). The total number of intersections was different between all groups (all P<0.05). Two-week-old neurons had fewer intersections than older adult-born neurons in both proximal and distal dendritic regions (60-130 μm, *P<0.05 vs 4w and 7w cells; 240-300 μm, *P<0.05 vs 24w cells). Neonatal-born neurons had more intersections in proximal dendritic regions (20-60 μm, *P<0.05 vs all other groups). Four-week-old neurons had fewer intersections than 7 and 24-week-old neurons at 100-150 μm (*P<0.05). Lines connect mean values (not shown), shading indicates s.e.m. e) Two-week-old adult-born neurons had more dendritic branches than all other groups except 24w cells. After initial pruning from 2w to 4w, the number of branches increased from 7w to 24w (Kruskal-Wallis test, P<0.0001 followed by Dunn's post-test). Symbols as in (b). f) Dendritic branching varied as a function of branch order and cell age (effect of cell age $F_{4,1682}$=7.1, P<0.0001; effect of dendrite order $F_{7,1682}$=394.1, P<0.0001, interaction $F_{28,1682}$=9.0, P<0.0001). Neonatal-born neurons, and older adult-born neurons, had more lower-order branches than younger adult-born neurons. In contrast, young adult-born neurons (particularly 2w) had more high-order branches. Bars indicate mean ± s.e.m. g) The branching index (branch tips / # primary dendrites) was greater in 2w cells than all other cell ages (Kruskal Wallis test P<0.0001). White, grey and black symbols indicate cells with 1, 2 and 3 primary dendrites, respectively. The branching index remained greater in 2w cells when only single primary dendrite cells were analyzed (ANOVA, $F_{4,170}$=13.3, P<0.0001; 2w vs all other groups P<0.05). *P<0.05, **P<0.01, ***P<0.001, ****P<0.0001.

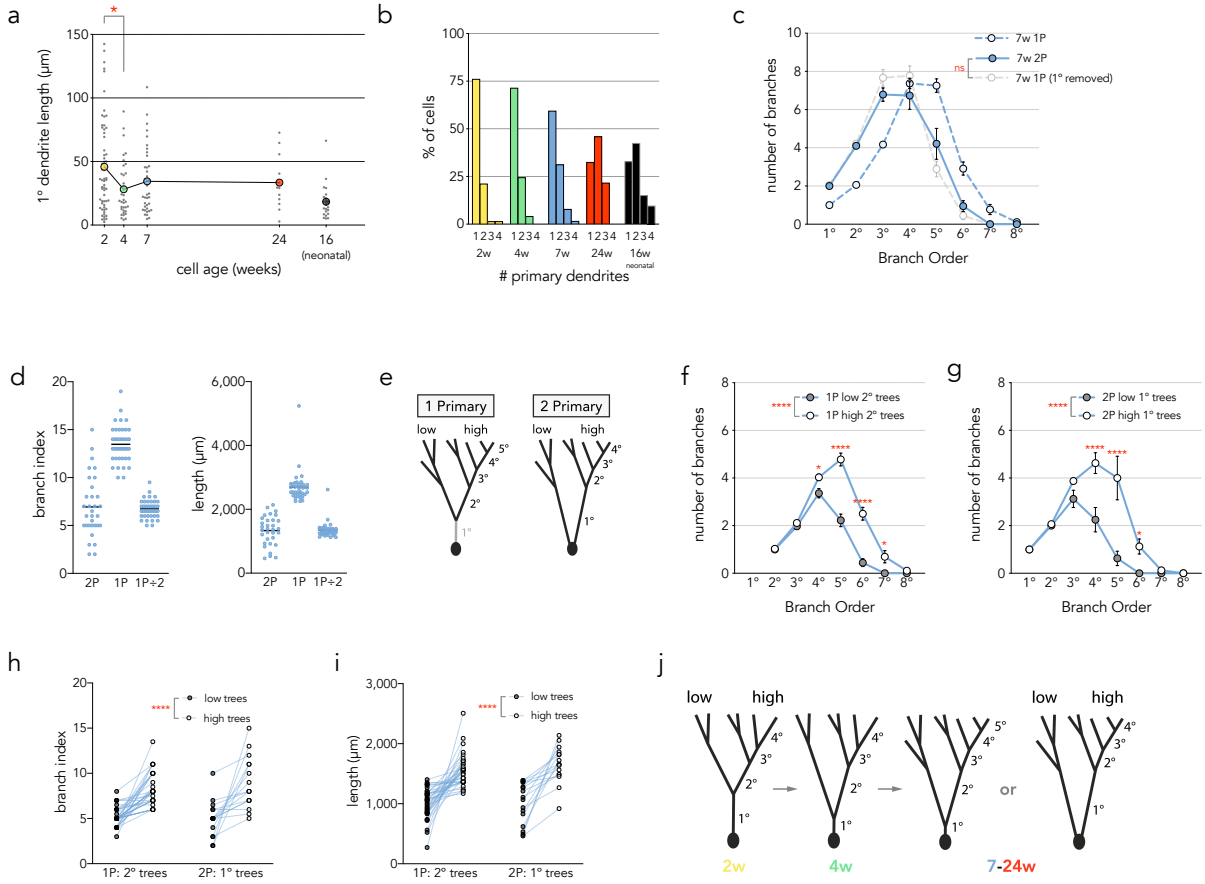


Figure 3: Unzipping model of primary dendrite formation. a) The primary dendrite shortens between 2-4 weeks of cell age (only includes cells with a single primary dendrite; $F_{4,167}$=5.1, P=0.0007). b) The number of primary dendrites per cell, by age. c) Dendritic branch orders are similar in 7w cells that have 1 and 2 primary dendrites (1P, 2P), once the number of primary dendrites is accounted for (7w 2P vs 7w 1P shifted, effect of cell type: $F_{1,35}$=0.03, P=0.9; cell type x branch order interaction, $F_{6,210}$=2.2, P=0.04, post hoc comparisons at each order all P>0.1). d) Primary dendritic trees on 7w cells with 2 primary dendrites (2P) displayed more variable degrees of maturation than cells with 1 primary dendrite (1P), as measured by branch index and total length. e) Schematic of approach for comparing branch-tree morphology in cells with 1 vs 2 primary dendrites. For 2P cells, the 2 primary dendrites and their respective trees were compared; "low" trees had fewer branches and shorter total length than "high" trees. For 1P cells, the 2 secondary dendrites and their respective trees were compared. f) 7w cells with 1 primary dendrite had one 2° dendritic tree that branched significantly less ("low") than the other ("high"; effect of cell type: $F_{1,35}$=53, P<0.0001; cell type x branch order interaction: $F_{6,210}$=24, P<0.0001). g) 7w cells with 2 primary dendrites had one 2° dendritic tree that branched significantly less than the other (effect of cell type: $F_{1,15}$=16, P<0.01; cell type x branch order interaction: $F_{7,105}$=9.8, P<0.0001). h) 7w cells had 2 main dendritic trees that differed in amount of branching, regardless of whether the cells had 1 or 2 primary dendrites (effect of tree type: $F_{1,50}$=67, P<0.0001; tree type x cell type interaction: $F_{1,50}$=1.0, P=0.3). i) "High" trees had greater total dendritic length than "low" trees, in both cells with 1 and 2 primary dendrites (effect of tree type: $F_{1,50}$=71, P<0.0001; tree type x cell type interaction: $F_{1,50}$=0.4, P=0.5). j)

Unzipping model: The dendritic tree of adult-born neurons is inherently variable, with some "sub-trees" having more branches than others. Most adult-born neurons begin with a single primary dendrite, which shortens as the first branch point moves closer to the soma. In many cells the first branch point reaches the soma causing the transition from 1 to 2 primary dendrites, and differential complexity carries over as 2°-based subtrees become 1°-based subtrees.

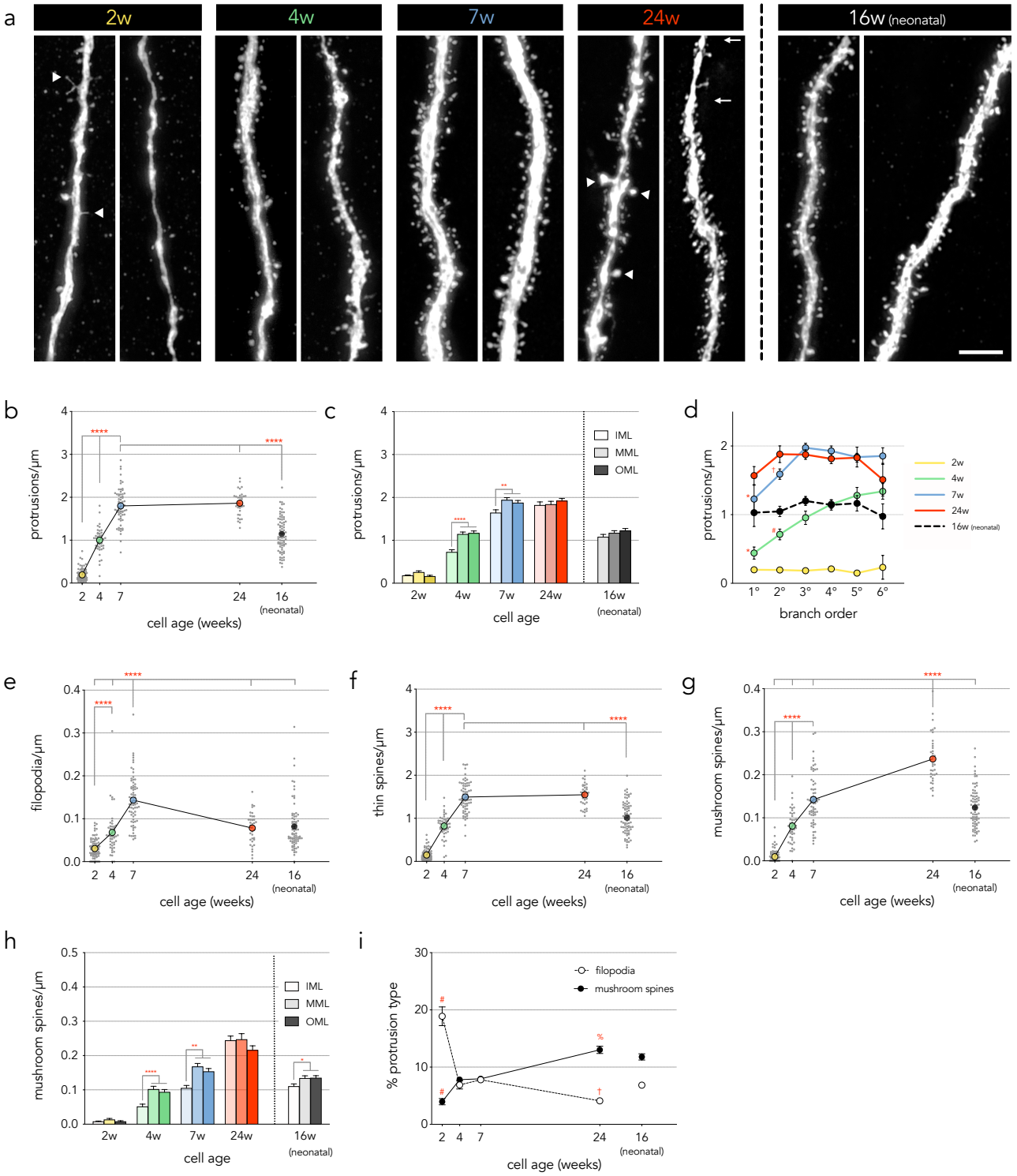


1

2 Figure 4: Protrusion densities in adult-born neurons reach and surpass that of neonatal-born neurons. a)
3 Confocal images of spines/protrusions; additional examples in Fig. 4-1. Filled arrowheads in the 2 week
4 example indicate filopodia; open arrowheads in the 24w example indicate mushroom spines; segment
5 identified by arrows at 24w demonstrates region of low spine density in the distal tip of a dendrite in the

outer molecular layer. Scale bar, 10 μm. b) Total protrusion densities increase with age in adult-born neurons, and plateaued by 7 weeks at levels that were greater than neonatal-born neurons ($F_{4,314}$=299, P<0.0001). c) Protrusion densities increased with cell age at a slower rate in the inner molecular layer than in the middle and outer molecular layers (cell age x layer interaction $F_{8,883}$=3.5, P=0.0005). d) In immature neurons, protrusion densities were reduced in lower-order dendrites (branch order x cell age interaction $F_{20,615}$=2.9, P<0.0001; 1° vs 3°,4°,5°,6° *P<0.05; 2° vs 4°,5°,6° $^{\#}$P<0.01; 2° vs 3°,4° $^{\dagger}$P<0.01). e) Filopodia densities increased from 2w to peak levels at 7w, and declined by 24w, which was not different that neonatally-born neurons ($F_{4,314=65}$, P<0.0001). Thin spines made up the majority of protrusions and increased over 7 weeks to levels that were greater than neonatally-born neurons ($F_{4,314}$=335, P<0.0001). g) Mushroom spine densities increased as adult-born neuron aged and, by 24 weeks, were greater than all other groups ($F_{4,314}$=201, P<0.0001). h) Mushroom spine densities increased with adult-born neuron age at a slower rate in the inner molecular layer. Mushroom spine densities were also lower in the inner molecular layer of neonatally-born neurons (cell age x subregion interaction ($F_{8,883}$=4.7, P<0.001). The proportion of filopodial protrusions was greatest in young cells and the proportion of mushroom was greatest in older cells (Kruskal-Wallis tests for both protrusion types, P<0.0001). Symbols and bars indicate means, error bars indicate s.e.m. IML: inner molecular layer, MML: middle molecular layer, OML: outer molecular layer. *P<0.05, **P<0.01, ***P<0.001, ****P<0.0001, $^{\#}$P<0.001 vs same protrusion type at all other ages, $^{\%}$P<0.0001 vs same protrusion type at 4w and 7w, $^{\dagger}$P<0.05 vs same protrusion type at 4w, 7w, 16w-neonatal. Bars indicate mean ± s.e.m.

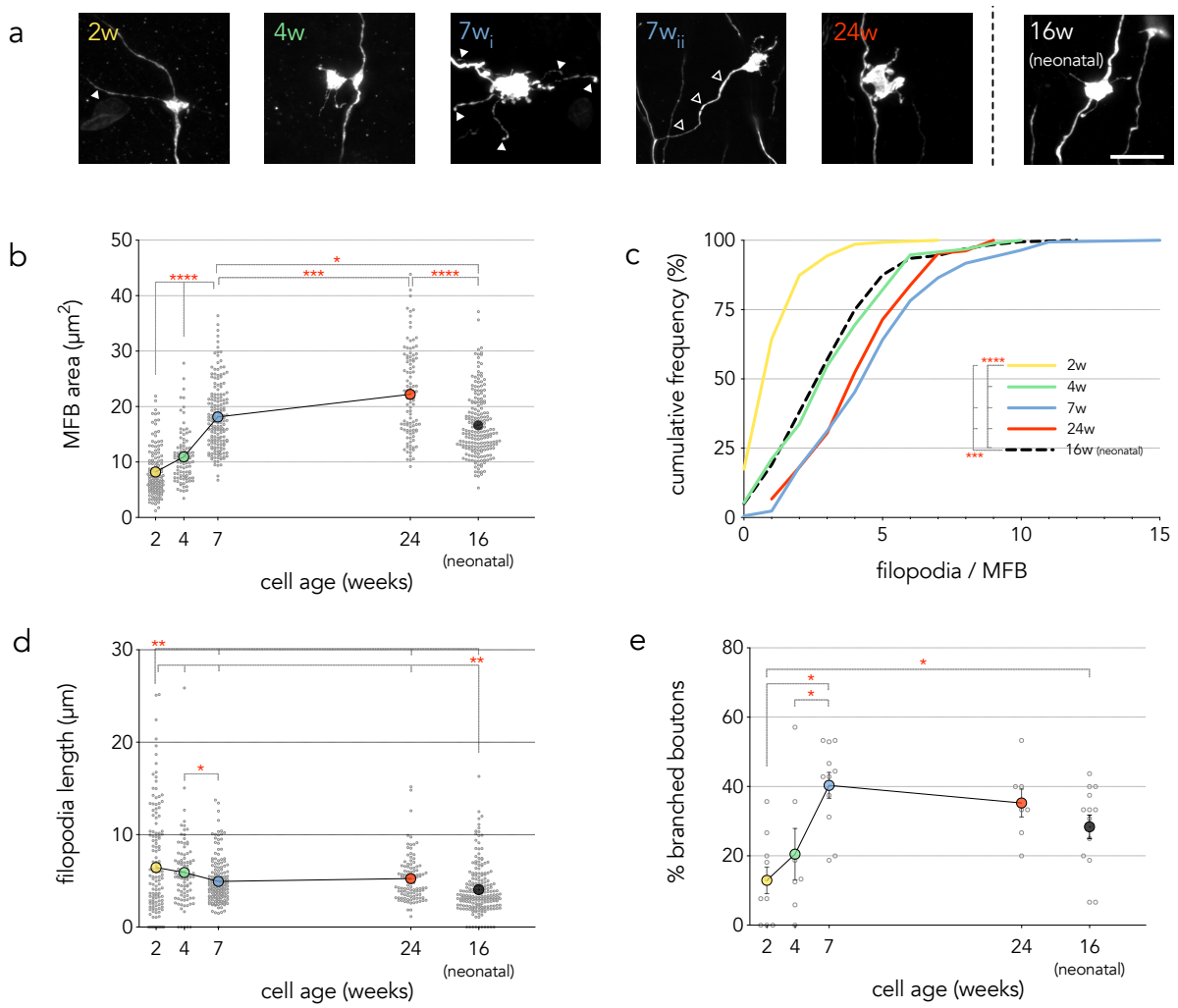


Figure 5: Efferent synaptic terminals of neonatally- and adult-born neurons. a) Confocal images of retrovirally-labelled mossy fiber boutons (MFB) and filopodial terminals. Z-stack videos of MFB examples are included as Videos 5-1 to 5-5. Filled arrowheads in 2w and $7w_i$ images indicate filopodial extensions. Open arrowheads in $7w_{ii}$ indicates a branched MFB. Scale bar, 10 μm for all images except for $7w_{ii}$, 11.7 μm. b) MFBs increased in size with cell age ($F_{4,708}$=160, P<0.0001). c) The number of filopodia per MFB increased from 2-7w and remained greater than neonatally-born neurons at 24w (Kruskal-Wallis test, P<0.0001). d) Filopodia length was greatest at 2w and decreased with cell age but remained longer than neonatally-born neurons ($F_{4,667}$=18, P<0.0001). e) The proportion of branched MFBs increased with cell age and did not differ significantly between older adult-born neurons and neonatal-born neurons ($F_{5,47}$=6, P<0.001). *P<0.05, **P<0.01, ***P<0.001, ****P<0.0001.

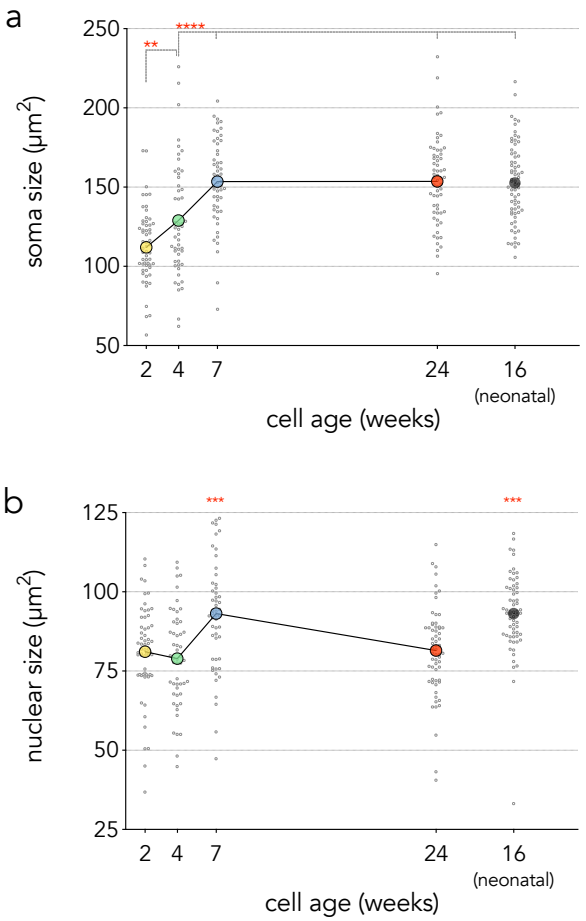


Figure 6: Soma and nuclear morphology. a) The cell soma increased in size as adult-born cells aged, plateauing and matching neonatal-born neurons by 7 weeks ($F_{4,289}$=27, P<0.0001; **P<0.01, ****P<0.0001). b) The nuclear size of adult-born neurons was generally consistent across cell ages, except at 7w when nuclear were larger and equivalent to neonatal-born neurons ($F_{4,291}$=12.5, P<0.0001). ***P<0.001 vs 2w, 4w and 24w.

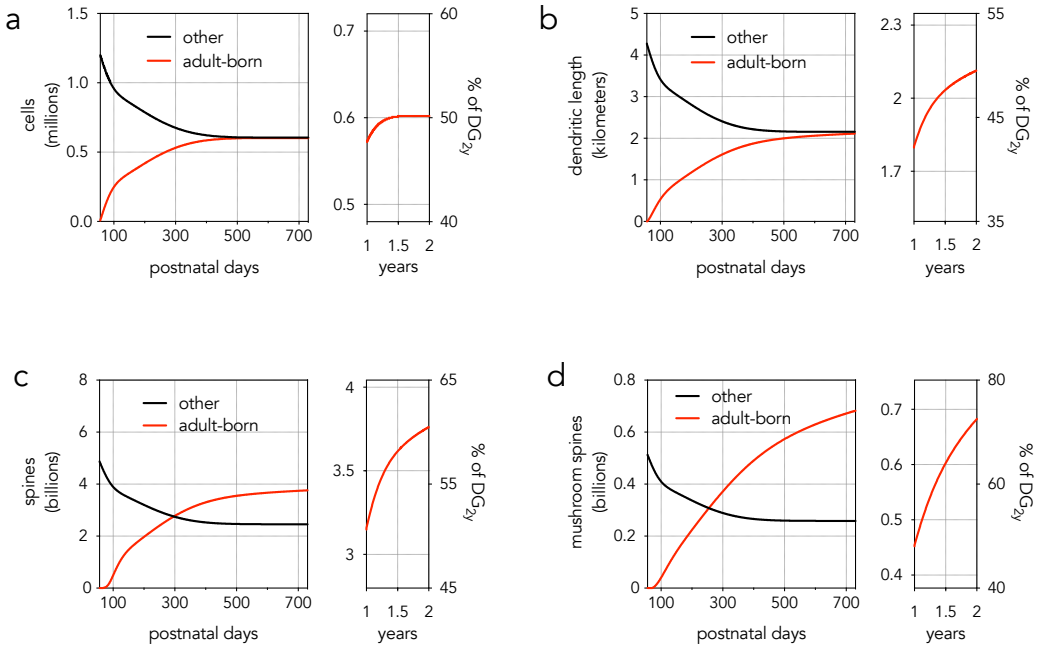


Figure 7: Modelling cumulative effects of adult neurogenesis. Square left panels show neurogenesis effects throughout the approximate full lifespan of a rat (2 years). Narrow right panels focus on cumulative effects during the 2nd half of life, when neurogenesis has declined but growth continues; right y-axis shows percent contribution by neurogenesis, relative to the total granule cell population at 2 years of life. Other/adult-born = cells born before/after 8 weeks of age. a) Adult-born neurons accumulate throughout the first 1.5 years of life and ultimately account for ~half the total granule cell population (numbers are unilateral. b) Total dendritic length contributed by adult neurogenesis increases throughout life, even though neurogenesis ends at 1.5 years in this model. c) Due to protracted growth of dendrites and spines, the total number of spines (thin + mushroom; c), and mushroom spines (d) added to the dentate gyrus increases through old age. Equations and code in Fig 7-1, summary statistics in Table 7-1.

# REFERENCES


Acsády L, Kamondi A, Sík A, Freund T, Buzsáki G (1998) GABAergic cells are the major postsynaptic targets of mossy fibers in the rat hippocampus. J Neurosci 18:3386–3403.

Aimone JB, Wiles J, Gage FH (2009) Computational influence of adult neurogenesis on memory encoding. Neuron 61:187–202.

Akers KG, Martinez-Canabal A, Restivo L, Yiu AP, De Cristofaro A, Hsiang H-L, Wheeler AL, Guskjolen A, Niibori Y, Shoji H, Ohira K, Richards BA, Miyakawa T, Josselyn SA, Frankland PW (2014) Hippocampal Neurogenesis Regulates Forgetting During Adulthood and Infancy. Science 344:598–602.

Altman J, Das GD (1965) Autoradiographic and histological evidence of postnatal hippocampal neurogenesis in rats. J Comp Neurol 124:319–335.

Alvarez DD, Giacomini D, Yang SM, Trinchero MF, Temprana SG, Büttner KA, Beltramone N, Schinder AF (2016) A disynaptic feedback network activated by experience promotes the integration of new granule cells. Science 354:459–465.

Amaral DG, Dent JA (1981) Development of the mossy fibers of the dentate gyrus: I. A light and electron microscopic study of the mossy fibers and their expansions. J Comp Neurol 195:51–86.

Ambrogini P, Cuppini R, Lattanzi D, Ciuffoli S, Frontini A, Fanelli M (2010) Synaptogenesis in adult-generated hippocampal granule cells is affected by behavioral experiences. Hippocampus 20:799–810.

Anderson ML, Sisti HM, Curlik DM II, Shors TJ (2010) Associative learning increases adult neurogenesis during a critical period. European Journal of Neuroscience 33:175–181.

Angevine JB (1965) Time of neuron origin in the hippocampal region. An autoradiographic study in the mouse. Exp Neurol Suppl:Suppl2:1–Suppl2:70.

Beining M, Jungenitz T, Radic T, Deller T, Cuntz H, Jedlicka P, Schwarzacher SW (2017) Adult-born dentate granule cells show a critical period of dendritic reorganization and are distinct from developmentally born cells. Brain structure & function 222:1427–1446.

Bergami M, Masserdotti G, Temprana SG, Motori E, Eriksson TM, Göbel J, Yang SM, Conzelmann K-K, Schinder AF, Götz M, Berninger B (2015) A critical period for experience-dependent remodeling of adult-born neuron connectivity. Neuron 85:710–717.

Berry KP, Nedivi E (2017) Spine Dynamics: Are They All the Same? Neuron 96:43–55.

Bird AD, Cuntz H (2016) Optimal Current Transfer in Dendrites. van Rossum MCW, ed. PLoS Comput Biol 12:e1004897.

Bolós M, Terreros-Roncal J, Perea JR, Pallas-Bazarra N, Ávila J, Llorens-Martín M (2019) Maturation dynamics of the axon initial segment (AIS) of newborn dentate granule cells in young adult C57BL/6J mice. J Neurosci:2253–18.

Cahill SP, Yu RQ, Green D, Todorova EV, Snyder JS (2017) Early survival and delayed death of developmentally-born dentate gyrus neurons. Hippocampus 49:553.

Cameron HA, Woolley CS, McEwen BS, Gould E (1993) Differentiation of newly born neurons and glia in the dentate gyrus of the adult rat. Neuroscience 56:337–344.

Chancey JH, Adlaf EW, Sapp MC, Pugh PC, Wadiche JI, Overstreet-Wadiche LS (2013) GABA Depolarization Is Required for Experience-Dependent Synapse Unsilencing in Adult-Born Neurons. J Neurosci 33:6614–6622.

Chancey JH, Poulsen DJ, Wadiche JI, Overstreet-Wadiche L (2014) Hilar Mossy Cells Provide the First Glutamatergic Synapses to Adult-Born Dentate Granule Cells. J Neurosci 34:2349–2354.

Chicurel ME, Harris KM (1992) Three-dimensional analysis of the structure and composition of CA3 branched dendritic spines and their synaptic relationships with mossy fiber boutons in the rat hippocampus. J Comp Neurol 325:169–182.

Claiborne BJ, Amaral DG, Cowan WM (1986) A light and electron microscopic analysis of the mossy fibers of the rat dentate gyrus. J Comp Neurol 246:435–458.

Coleman PD, Flood DG (1987) Neuron numbers and dendritic extent in normal aging and Alzheimer's disease. Neurobiology of Aging 8:521–545.

Dayer AG, Ford AA, Cleaver KM, Yassaee M, Cameron HA (2003) Short-term and long-term survival of new neurons in the rat dentate gyrus. J Comp Neurol 460:563–572.

De Paola V, Holtmaat A, Knott G, Song S, Wilbrecht L, Caroni P, Svoboda K (2006) Cell type-specific structural plasticity of axonal branches and boutons in the adult neocortex. Neuron 49:861–875.

DeCarolis NA, Mechanic M, Petrik D, Carlton A, Ables JL, Malhotra S, Bachoo R, Götz M, Lagace DC, Eisch AJ (2013) In vivo contribution of nestin- and GLAST-lineage cells to adult hippocampal neurogenesis. Hippocampus 23:708–719.

Dennis CV, Suh LS, Rodriguez ML, Kril JJ, Sutherland GT (2016) Human adult neurogenesis across the ages: An immunohistochemical study. Neuropathol Appl Neurobiol 42:621–638.

Diamantaki M, Frey M, Berens P, Preston-Ferrer P, Burgalossi A (2016) Sparse activity of identified dentate granule cells during spatial exploration. eLife 5:e20252.

Dieni CV, Nietz AK, Panichi R, Wadiche JI, Overstreet Wadiche L (2013) Distinct Determinants of Sparse Activation during Granule Cell Maturation. J Neurosci 33:19131–19142.

Drew LJ, Kheirbek MA, Luna VM, Denny CA, Cloidt MA, Wu MV, Jain S, Scharfman HE, Hen R (2015) Activation of local inhibitory circuits in the dentate gyrus by adult-born neurons. Hippocampus.

Engel D, Jonas P (2005) Presynaptic action potential amplification by voltage-gated Na+ channels in hippocampal mossy fiber boutons. Neuron 45:405–417.

Epp JR, Spritzer MD, Galea LAM (2007) Hippocampus-dependent learning promotes survival of new neurons in the dentate gyrus at a specific time during cell maturation. Neuroscience 149:273–285.

Eriksson PS, Perfilieva E, Björk-Eriksson T, Alborn AM, Nordborg C, Peterson DA, Gage FH (1998) Neurogenesis in the adult human hippocampus. Nat Med 4:1313–1317.

Faulkner RL, Jang M-H, Liu X-B, Duan X, Sailor KA, Kim JY, Ge S, Jones EG, Ming G-L, Song H, Cheng H-J (2008) Development of hippocampal mossy fiber synaptic outputs by new neurons in the adult brain. Proceedings of the National Academy of Sciences 105:14157–14162.

Feldman LA, Shapiro ML, Nalbantoglu J (2010) A novel, rapidly acquired and persistent spatial memory task that induces immediate early gene expression. Behavioral and brain functions : BBF 6:35.

Flood DG, Buell SJ, Defiore CH, Horwitz GJ, Coleman PD (1985) Age-related dendritic growth in dentate gyrus of human brain is followed by regression in the 'oldest old'. Brain Res 345:366–368.

Galimberti I, Bednarek E, Donato F, Caroni P (2010) EphA4 signaling in juveniles establishes topographic specificity of structural plasticity in the hippocampus. Neuron 65:627–642.

Galimberti I, Gogolla N, Alberi S, Santos AF, Muller D, Caroni P (2006) Long-Term Rearrangements of Hippocampal Mossy Fiber Terminal Connectivity in the Adult Regulated by Experience. Neuron 50:749–763.

Ge S, Yang C-H, Hsu K-S, Ming G-L, Song H (2007) A Critical Period for Enhanced Synaptic Plasticity in Newly Generated Neurons of the Adult Brain. Neuron 54:559–566.

Gonçalves JT, Bloyd CW, Shtrahman M, Johnston ST, Schafer ST, Parylak SL, Tran T, Chang T, Gage FH (2016) In vivo imaging of dendritic pruning in dentate granule cells. Nat Neurosci.

Gu Y, Arruda-Carvalho M, Wang J, Janoschka SR, Josselyn SA, Frankland PW, Ge S (2012) Optical controlling reveals time-dependent roles for adult-born dentate granule cells. Nat Neurosci 15:1700–1706.

Guo N, Soden ME, Herber C, Kim MT, Besnard A, Lin P, Ma X, Cepko CL, Zweifel LS, Sahay A (2018) Dentate granule cell recruitment of feedforward inhibition governs engram maintenance and remote memory generalization. Nature Publishing Group 24:438–449.

Henze DA, Wittner L, Buzsáki G (2002) Single granule cells reliably discharge targets in the hippocampal CA3 network in vivo. Nat Neurosci 5:790–795.

Holtmaat A, Svoboda K (2009) Experience-dependent structural synaptic plasticity in the mammalian brain. Nat Rev Neurosci 10:647–658.

Imura T, Kobayashi Y, Suzutani K, Ichikawa-Tomikawa N, Chiba H (2018) Differential expression of a stress-regulated gene Nr4a2 characterizes early- and late-born hippocampal granule cells. Hippocampus:1–38.

Jessberger S, Zhao C, Toni N, Clemenson GD, Li Y, Gage FH (2007) Seizure-associated, aberrant neurogenesis in adult rats characterized with retrovirus-mediated cell labeling. J Neurosci 27:9400–9407.

Jungenitz T, Beining M, Radic T, Deller T, Cuntz H, Jedlicka P, Schwarzacher SW (2018) Structural homo- and heterosynaptic plasticity in mature and adult newborn rat hippocampal granule cells. Proceedings of the National Academy of Sciences 85:201801889.

Kerloch T, Clavreul S, Goron A, Abrous DN, Pacary E (2018) Dentate Granule Neurons Generated During Perinatal Life Display Distinct Morphological Features Compared With Later-Born Neurons in the Mouse Hippocampus. Cerebral Cortex 301:365.

Kim WR, Christian K, Ming G-L, Song H (2012) Time-dependent involvement of adult-born dentate granule cells in behavior. Behav Brain Res 227:470–479.

Knoth R, Singec I, Ditter M, Pantazis G, Capetian P, Meyer RP, Horvat V, Volk B, Kempermann G (2010) Murine features of neurogenesis in the human hippocampus across the lifespan from 0 to 100 years. PLoS ONE 5:e8809.

Kole MHP, Ilschner SU, Kampa BM, Williams SR, Ruben PC, Stuart GJ (2008) Action potential generation requires a high sodium channel density in the axon initial segment. Nat Neurosci 11:178–186.

Kuhn HG, Dickinson-Anson H, Gage FH (1996) Neurogenesis in the dentate gyrus of the adult rat: age-related decrease of neuronal progenitor proliferation. J Neurosci 16:2027–2033.

Laplagne DA, Espósito MS, Piatti VC, Morgenstern NA, Zhao C, van Praag H, Gage FH, Schinder AF (2006) Functional convergence of neurons generated in the developing and adult hippocampus. PLoS Biol 4:e409.

Lazic SE (2012) Modeling hippocampal neurogenesis across the lifespan in seven species. Neurobiol Aging 33:1664–1671.

Leal SL, Yassa MA (2015) Neurocognitive Aging and the Hippocampus across Species. Trends Neurosci 38:800–812.

Lee H, Wang C, Deshmukh SS, Knierim JJ (2015) Neural Population Evidence of Functional Heterogeneity along the CA3 Transverse Axis: Pattern Completion versus Pattern Separation. Neuron.

Lemaire V, Tronel S, Montaron M-F, Fabre A, Dugast E, Abrous DN (2012) Long-lasting plasticity of hippocampal adult-born neurons. J Neurosci 32:3101–3108.

Leranth C, Hajszan T (2007) Extrinsic afferent systems to the dentate gyrus. Prog Brain Res 163:63–84.

Longair MH, Baker DA, Armstrong JD (2011) Simple Neurite Tracer: open source software for reconstruction, visualization and analysis of neuronal processes. Bioinformatics 27:2453–2454.

Losonczy A, Makara JK, Magee JC (2008) Compartmentalized dendritic plasticity and input feature storage in neurons. Nature 452:436–441.

Marín-Burgin A, Mongiat LA, Pardi MB, Schinder AF (2012) Unique processing during a period of high excitation/inhibition balance in adult-born neurons. Science 335:1238–1242.

McBain CJ (2008) Differential mechanisms of transmission and plasticity at mossy fiber synapses. Prog Brain Res 169:225–240.

Mongiat LA, Espósito MS, Lombardi G, Schinder AF (2009) Reliable activation of immature neurons in the adult hippocampus. PLoS ONE 4:e5320.

Moreno-Jiménez EP, Flor-García M, Terreros-Roncal J, Rábano A, Cafini F, Pallas-Bazarra N, Avila J, Llorens-Martín M (2019) Adult hippocampal neurogenesis is abundant in neurologically healthy subjects and drops sharply in patients with Alzheimer's disease. Nature Publishing Group 108:621.

Niibori Y, Yu T-S, Epp JR, Akers KG, Josselyn SA, Frankland PW (2012) Suppression of adult neurogenesis impairs population coding of similar contexts in hippocampal CA3 region. Nat Comms 3:1253.

Ofer N, Shefi O, Yaari G (2017) Branching morphology determines signal propagation dynamics in neurons. Sci Rep 7:1–9.

Ohkawa N, Saitoh Y, Tokunaga E, Nihonmatsu I, Ozawa F, Murayama A, Shibata F, Kitamura T, Inokuchi K (2012) Spine formation pattern of adult-born neurons is differentially modulated by the induction timing and location of hippocampal plasticity. Dunaevsky A, ed. PLoS ONE 7:e45270.

Ohline SM, Wake KL, Hawkridge M-V, Dinnunhan MF, Hegemann RU, Wilson A, Schoderboeck L, Logan BJ, Jungenitz T, Schwarzacher SW, Hughes SM, Abraham WC (2018) Adult-born dentate granule cell excitability depends on the interaction of neuron age, ontogenetic age and experience. Brain structure & function 383:335.

Overstreet-Wadiche LS, Bensen AL, Westbrook GL (2006) Delayed development of adult-generated granule cells in dentate gyrus. J Neurosci 26:2326–2334.

Restivo L, Niibori Y, Mercaldo V, Josselyn SA, Frankland PW (2015) Development of Adult-Generated Cell Connectivity with Excitatory and Inhibitory Cell Populations in the Hippocampus. J Neurosci 35:10600–10612.

Rollenhagen A, Sätzler K, Rodriguez EP, Jonas P, Frotscher M, Lübke JHR (2007) Structural determinants of transmission at large hippocampal mossy fiber synapses. J Neurosci 27:10434–10444.

Rolls ET (2010) A computational theory of episodic memory formation in the hippocampus. Behav Brain Res 215:180–196.

Rowan MJM, DelCanto G, Yu JJ, Kamasawa N, Christie JM (2016) Synapse-Level Determination of Action Potential Duration by K+ Channel Clustering in Axons. Neuron 91:370–383.

Ruediger S, Vittori C, Bednarek E, Genoud C, Strata P, Sacchetti B, Caroni P (2011) Learning-related feedforward inhibitory connectivity growth required for memory precision. Nature 473:514–518.

Save L, Baude A, Cossart R (2018) Temporal Embryonic Origin Critically Determines Cellular Physiology in the Dentate Gyrus. Cerebral Cortex 32:6688.

Schlessinger AR, Cowan WM, Gottlieb DI (1975) An autoradiographic study of the time of origin and the pattern of granule cell migration in the dentate gyrus of the rat. J Comp Neurol 159:149–175.

Schmidt-Hieber C, Jonas P, Bischofberger J (2004) Enhanced synaptic plasticity in newly generated granule cells of the adult hippocampus. Nature 429:184–187.

Seress L (1992) Morphological variability and developmental aspects of monkey and human granule cells: differences between the rodent and primate dentate gyrus. Epilepsy Res Suppl 7:3–28.

Seress L, Frotscher M (1990) Morphological variability is a characteristic feature of granule cells in the primate fascia dentata: a combined Golgi/electron microscope study. J Comp Neurol 293:253–267.

Snyder JS (2019) Recalibrating the Relevance of Adult Neurogenesis. Trends Neurosci:1–15.

Snyder JS, Cameron HA (2012) Could adult hippocampal neurogenesis be relevant for human behavior? Behav Brain Res 227:384–390.

Snyder JS, Choe JS, Clifford MA, Jeurling SI, Hurley P, Brown A, Kamhi JF, Cameron HA (2009) Adult-born hippocampal neurons are more numerous, faster maturing, and more involved in behavior in rats than in mice. J Neurosci 29:14484–14495.

Snyder JS, Kee N, Wojtowicz JM (2001) Effects of adult neurogenesis on synaptic plasticity in the rat dentate gyrus. J Neurophysiol 85:2423–2431.

Sorrells SF, Paredes MF, Cebrian-Silla A, Sandoval K, Qi D, Kelley KW, James D, Mayer S, Chang J, Auguste KI, Chang EF, Gutierrez AJ, Kriegstein AR, Mathern GW, Oldham MC, Huang EJ, García-Verdugo JM, Yang Z, Alvarez-Buylla A (2018) Human hippocampal neurogenesis drops sharply in children to undetectable levels in adults. Nature 555:377–381.

Spruston N (2008) Pyramidal neurons: dendritic structure and synaptic integration. Nat Rev Neurosci 9:206–221.

Stone SSD, Teixeira CM, Zaslavsky K, Wheeler AL, Martinez-Canabal A, Wang AH, Sakaguchi M, Lozano AM, Frankland PW (2011) Functional convergence of developmentally and adult-generated granule cells in dentate gyrus circuits supporting hippocampus-dependent memory. Hippocampus 21:1348–1362.

Sun GJ, Sailor KA, Mahmood QA, Chavali N, Christian KM, Song H, Ming G-L (2013) Seamless reconstruction of intact adult-born neurons by serial end-block imaging reveals complex axonal guidance and development in the adult hippocampus. J Neurosci 33:11400–11411.

Todorova EV, Cahill SP, O'Leary T, Snyder JS (2017) Stressful experiences differentially regulate immediate-early genes and stress hormone receptors in immature and mature dentate gyrus neurons. Matters Select:1–6.

Toni N, Laplagne DA, Zhao C, Lombardi G, Ribak CE, Gage FH, Schinder AF (2008) Neurons born in the adult dentate gyrus form functional synapses with target cells. Nat Neurosci 11:901–907.

Toni N, Teng EM, Bushong EA, Aimone JB, Zhao C, Consiglio A, van Praag H, Martone ME, Ellisman MH, Gage FH (2007) Synapse formation on neurons born in the adult hippocampus. Nat Neurosci 10:727–734.

Trinchero MF, Büttner KA, Sulkes Cuevas JN, Temprana SG, Fontanet PA, Monzón-Salinas MC, Ledda F, Paratcha G, Schinder AF (2017) High Plasticity of New Granule Cells in the Aging Hippocampus. Cell Rep 21:1129–1139.

Tronel S, Fabre A, Charrier V, Oliet SHR, Gage FH, Abrous DN (2010) Spatial learning sculpts the dendritic arbor of adult-born hippocampal neurons. Proceedings of the National Academy of Sciences 107:7963–7968.

Tronel S, Lemaire V, Charrier V, Montaron M-F, Abrous DN (2015) Influence of ontogenetic age on the role of dentate granule neurons. Brain structure & function 220:645–661.

van Praag H, Schinder AF, Christie BR, Toni N, Palmer TD, Gage FH (2002) Functional neurogenesis in the adult hippocampus. Nature 415:1030–1034.

Vivar C, Peterson BD, van Praag H (2015) Running rewires the neuronal network of adult-born dentate granule cells. Neuroimage 131:29–41.

Vyleta NP, Borges-Merjane C, Jonas P (2016) Plasticity-dependent, full detonation at hippocampal mossy fiber-CA3 pyramidal neuron synapses. eLife 5:3386.

West MJ, Slomianka L, Gundersen HJ (1991) Unbiased stereological estimation of the total number of neurons in thesubdivisions of the rat hippocampus using the optical fractionator. Anat Rec 231:482–497.

Williams RS, Matthysse S (1983) Morphometric analysis of granule cell dendrites in the mouse dentate gyrus. J Comp Neurol 215:154–164.

Witter MP (2007) The perforant path: projections from the entorhinal cortex to the dentate gyrus. Prog Brain Res 163:43–61.

Zhao C, Teng EM, Summers RG, Ming G-L, Gage FH (2006) Distinct Morphological Stages of Dentate Granule Neuron Maturation in the Adult Mouse Hippocampus. J Neurosci 26:3–11.